Supporting Information

From Slicates to Oxonitridosilicates: Improving Optical Anisotropy for Phase-Matching as Ultraviolet Nonlinear Optical Materials

Xiaodong Zhang,[a] Lichao Guo, [a] Bingbing Zhang,[a]* Jin Yu,[a] Ying Wang,[a] Kui Wu,[a]* Hai-jun Wang,[a] and Ming-Hsien Lee[b]

[a]College of Chemistry and Environmental Science, Key Laboratory of Medicinal Chemistry and Molecular Diagnosis of the Ministry of Education, Chemical Biology Key Laboratory of Hebei Province, Hebei University, Baoding 071002, China.

[b]Department of Physics, Tamkang University, New Taipei City 25137, Taiwan.

Si_2N_2O: The crystal structure of Si_2N_2O is orthorhombic ($Cmc2_1$). It is isostructural with Ge_2N_2O.[41,57] The structure consists of the distorted SiN_3O tetrahedra linked with N atoms in the *bc* plane and further lingked by corner-sharing O atoms along the *a* axis forming a α-quartz-like 3D network structure. All the N atoms in the cell are three-coordinated with Si atoms that eleminate the 2*p* dangling bonds of N atoms and result in a large band gap E_g-HSE of 6.49 eV. The band structure show it has a indirect band gap (Figure S3(a)). Si and N atoms linked up into puckered hexagonal two-dimensional layers that arise a large birfingence (Δn=0.102 at 1064 nm). The calculated refractive index are in agreement with above analysis (Figure S3(b)). In additiaon, the calculated SHG coefficients of Si_2N_2O are $\chi_{113}=-1.615$, $\chi_{223}=-2.123$, and $\chi_{333}=2.557$ pm/V. The largest tensor χ_{333} is about 3.3 times that of d_{36}(KDP). The PDOS (Figure S3(c)) and SHG density (Figure S3(d)) analysis show that the occupied non-bonding 2*p* orbitals of N and O atoms, unoccupied anti-σ bonds in $SiON_3$ tetrahedra make the dominant contribution.

LiSiON: The structure of LiSiON is isostructural with KGeON[58] in which Li^+ cations are inserted in $[Si_2O_2N_2]^{2-}$ layers. The $[Si_2O_2N_2]^{2-}$ layers could be evolved from Si_2N_2O by splitting each O atom into two. It has an indirect band gap as shown in its band structures in Figure S4(a). The calculated E_g-HSE is 6.95 eV that is slightly larger than that of LiSiON. The birefringence of LiSiON is 0.060 at 1064 nm that is appropriate to achieving phase-matching (Figure S4(b)). The largest SHG tensor is χ_{223} (1.710 pm/V) that is about 2.2 times that of d_{36}(KDP). Similar with Si_2N_2O, $SiON_3$ tetrahedra make the dominant contribution to χ_{223} as shown in their PDOS (Figure S4(c)) and SHG density (Figure S4(d)). While Li^+ cations have no obvious contribution to SHG coefficient.

Table S1. Structures and calculated dipole moment (P_0), polarizability (α), polarizability anisotropy (δ), hyperpolarizability (β), and HOMO–LUMO gap (E_g) of $(SiN_xO_{4-x})^{(4+x)-}$ (x=0,1,2,3,4) anionic groups. Among them, $(SiN_3O)^{5-}$ and $(SiNO_3)^{7-}$ have the same point group symmetry *C*3v. Therefore, their polarized ellipsoidal bodies are spheroid. For the $(SiN_3O)^{5-}$, the maximum polarizability is perpendicular to the three-fold axis. As to the $(SiNO_3)^{7-}$, the maximum polarizability is in the direction of the three-fold axis. The symmetry of $(SiN_2O_2)^{6-}$ is *C*2v where the polarized ellipsoidal body is tri-axial ellipsoid. The maximum polarizability is along the direction determined by linking the two N atoms, while the minimum polarizability is in the direction determined by linking the two O atoms.

Groups	Structure	P_0	α	δ	β	E_g (eV)
$(SiO_4)^{4-}$	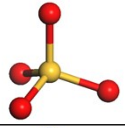	0 0 0	α_{xx}=34.2, α_{yy}=34.2, α_{zz}=34.2	0	$\beta_{xxx}=-\beta_{xyy}=-23.0$ $\beta_{xxz}=\beta_{yyz}=16.3$ $\beta_{zzz}=-32.1$	6.71
$(SiN_4)^{8-}$	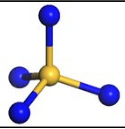	0 0 0	α_{xx}=69.9, α_{yy}=69.9, α_{zz}=69.9	0	$\beta_{xxx}=-\beta_{xyy}=-17.9$ $\beta_{xxz}=\beta_{yyz}=12.8$ $\beta_{zzz}=-24.3$	3.52
$(SiN_3O)^{7-}$	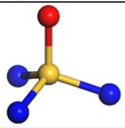	0, 0, 1.96	α_{xx}=66.1, α_{yy}=66.1, α_{zz}=60.9	5.2	$\beta_{xxx}=-\beta_{xyy}=27.3$ $\beta_{xxz}=\beta_{yyz}=110.1$ $\beta_{zzz}=116.3$	3.36
$(SiN_2O_2)^{6-}$	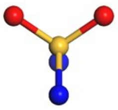	0., 0., 2.20	α_{xx}=51.5, α_{yy}=58.9, α_{zz}=60.5	9.0	β_{xxz}=4.3, β_{yyz}=60.4, β_{zzz}=357.1	3.77
$(SiNO_3)^{5-}$	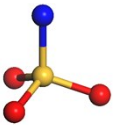	0 0 −1.96	α_{xx}=45.9 α_{yy}=45.9 α_{zz}=50.7	4.8	$\beta_{xxx}=-\beta_{xyy}=-105.5$ $\beta_{xxz}=\beta_{yyz}=-131.4$ $\beta_{zzz}=-254.5$	4.23

Table S2. The chemical formula, ICSD collection numbers, space groups (SG), calculated band gaps both using GGA and HSE (E_g-GGA and E_g-HSE, units: eV), birefringences (Δn) at 1064 nm, SHG coefficients ($\chi^{(2)}$) with scissors correction of selected silicates. Note the scissors operators that are used to correct Δn and $\chi^{(2)}$ are set as the difference between E_g-HSE and E_g-GGA.

Formula	ICSD	SG	E_g-GGA	E_g-HSE	Δn	$\chi^{(2)}$ (pm/V) (+sci.)
α-SiO_2	29122	$P3_12$	6.03	7.69	0.0085[#,a]	d_{11}(1.064 nm)=0.30 pm/V[#,b]
Li_3AlSiO_5	252215	$Pna2_1$	5.16	6.60	0.010	$\chi_{113}=0.025$; $\chi_{223}=0.363$; $\chi_{333}=-2.064$
$Sr_2MgSi_2O_7$	183978	$P\text{-}42_1\text{m}$	4.77	6.06	0.016	$\chi_{123}=-0.225$
$Rb_2Be_2Si_2O_7$	828	$P\text{nn}2$	4.28	5.86	0.011	$\chi_{113}=0.306$; $\chi_{223}=-0.508$; $\chi_{333}=-0.072$
$Sr_2ZnSi_2O_7$	247476	$P\text{-}42_1\text{m}$	4.18	5.70	0.004	$\chi_{123}=-1.414$

[#] The values are experimentally measured.

[a] G. Ghosh, *Opt. Commun.*, 1999, **163**, 95–102

[b] K. Hagimoto and A. Mito, *Appl. Opt.*, 1995, **34**, 8276–8282.

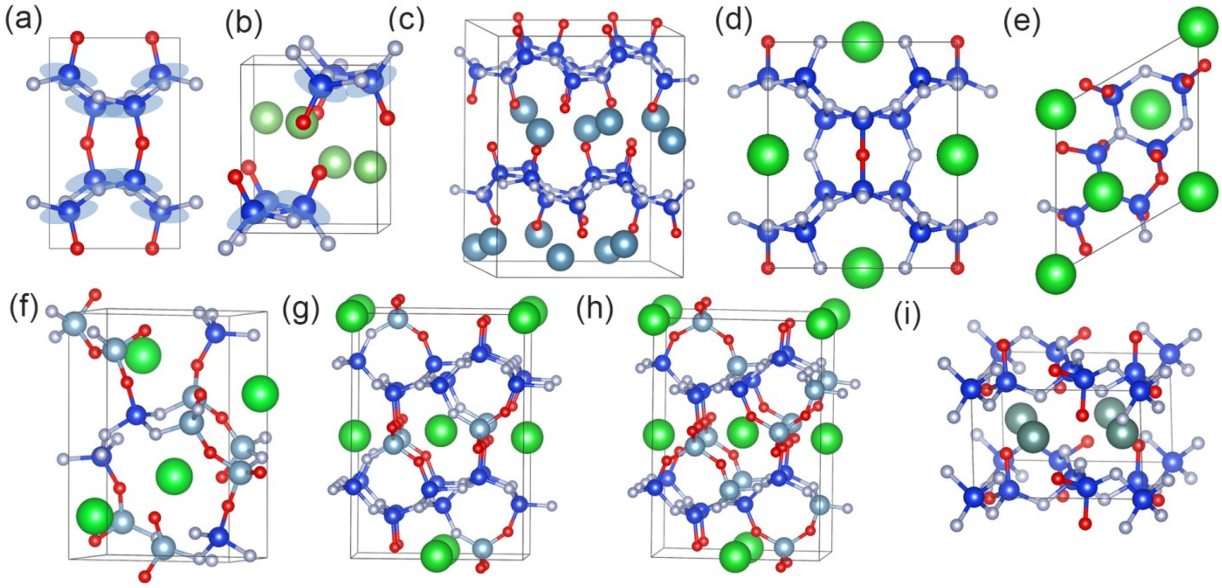

Figure S1. The crystal structures of (a) Si_2N_2O, (b) LiSiON, (c) $CaSi_2O_2N_2$, (d) $BaSi_6N_8O$, (e) $Ba_3Si_6O_9N_4$, (f) $SrSiAl_2N_2O_3$ (g) $Ba(AlSi_4)O_3N_5$, (h) $Ba(Al_2Si_3)N_4O_4$, and (i) $Y_2Si_3O_3N_4$. The blue, red, grey, and sky-blue balls connected by sticks are Si, O, N, and Al atoms, respectively. The isolated balls are cations as shown in their formulas. The circle planes in (a) and (b) represent the maximum polarizability plane of $SiON_3$ tetrahedra.

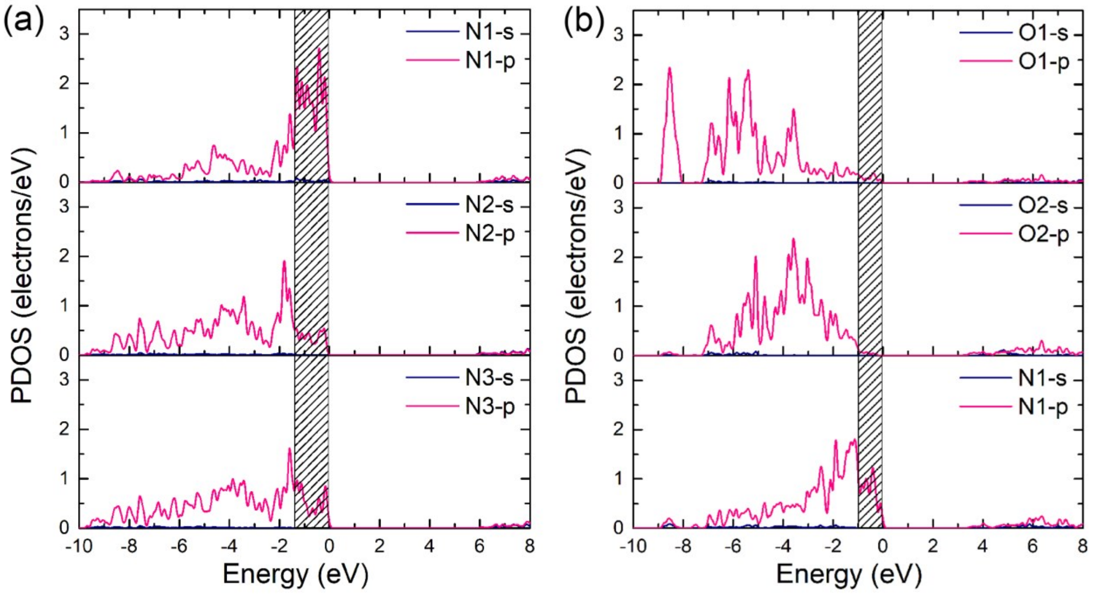

Figure S2. Partial density of states (PDOS) of N and O atoms in (a) $BaSi_6N_8O$ and (b) $Y_2Si_3O_3N_4$. In $BaSi_6N_8O$, N1 are two-coordinated, N2 and N3 atoms are three-coordinated. Non-bonding 2*p* orbitals of three-coordinated N atoms are obviously eliminated in the marked region compared with two-coordinated N atoms. In $Y_2Si_3O_3N_4$, two-coordinated N1 atoms contribute more electrons than that of bridge O1 atoms and terminal O2 atoms and as a result reduce its band gap.

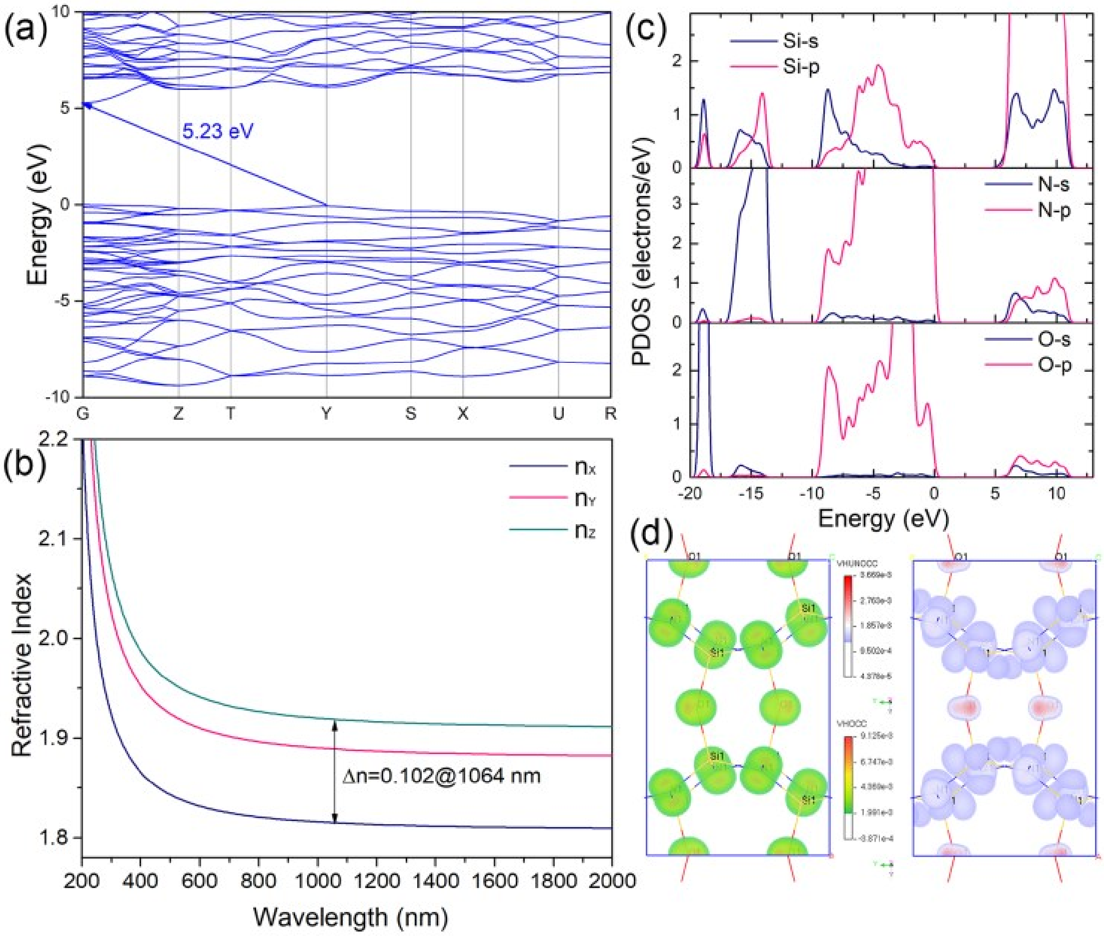

Figure S3. (a) The band structures calculated by using GGA-PBE functional, (b) refractive index along principle optical axes x, y, and z axies, (c) partial density of states (PDOS), and (d) occupied (left) and unoccupied (right) SHG density of virtual-hole (VH) processes for χ_{333} tensor of Si_2N_2O.

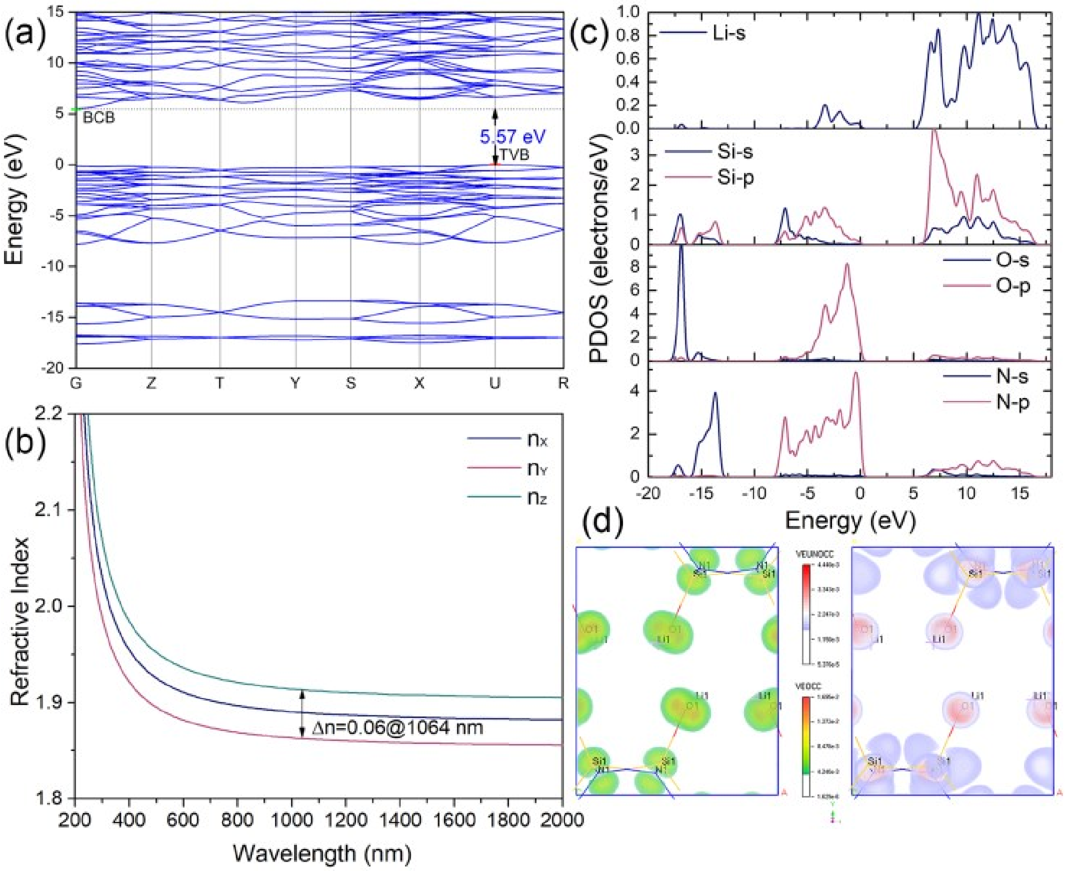

Figure S4. (a) The band structures calculated by using GGA-PBE functional, (b) refractive index along principle optical axes x, y, and z axies, (c) partial density of states (PDOS), and (d) occupied (left) and unoccupied (right) SHG density of virtual-electron (VE) processes of LiSiNO.